

# Dzyaloshinskii–Moriya interaction induced domain wall depinning anomaly in ferromagnetic nanowire

Han Kheng Teoh, Sarjoosing Goolaup and Wen Siang Lew

School of Physical and Mathematical Sciences, Nanyang Technological University, 637371, Singapore

E-mail: [wensiang@ntu.edu.sg](mailto:wensiang@ntu.edu.sg)

Received 21 April 2016, revised 26 September 2016

Accepted for publication 19 October 2016

Published 23 November 2016



## Abstract

Magnetic domain wall positional manipulation is usually through the introduction of potential trap. In this work, we show that the presence of interfacial Dzyaloshinskii–Moriya interaction leads to a different static depinning field for Néel domain walls with the same handedness in a notched magnetic nanowire. The difference in static depinning field is due to the Néel domain wall spin orientation. The spin orientation leads to different torques being exerted on the localized magnetic moments. This inherently imposes a spin orientation dependent diode-like behavior for domain walls in a notched nanowire. An equation which relates the difference in static depinning field to the notch geometry is derived. Micromagnetic simulation with varying damping constant reveals the influence of damping constant on the strength of depinning anomaly.

Keywords: Dzyaloshinskii–Moriya interaction, micromagnetism, domain wall

(Some figures may appear in colour only in the online journal)

## 1. Introduction

The control of magnetic domain wall (DW) position in nanoscale ferromagnetic structure is crucial for the successful realization of DW based magnetic logic and memory devices [1–5]. Interfacial Dzyaloshinskii–Moriya (IDM) interaction which accounts for asymmetric exchange interaction in magnetic system [6–12] has received renewed interest due to its role in favoring chiral structure in DWs, skyrmions and spin spirals [13–18]. These chiral structures possess intriguing magnetic behaviours such as asymmetric expansion of circular DW under field driving [19], large DW surface tilting [20], efficient DW driving with the application of magnetic field [21] or spin-polarized current [22] and suppression of Walker breakdown with strong IDM interaction [23]. DM interaction could lead to the possibility of controlling DW position electrically [24]. The presence of electric field changes the strength of Dzyaloshinskii–Moriya interaction which in turn changes the pinning potential on spin spiral DW. This provides a new means to pin a DW. Aforementioned studies on DWs have been performed in a uniform nanowire. The influence of IDM

interaction on DWs in a notched ultra-thin nanowire, which would likely be used to manipulate DWs in magnetic memory or logic devices, remains unexplored. In this paper, we theoretically and numerically show that irrespective of the type of notch, the presence of IDM interaction leads to different static depinning field for Néel DWs with similar handedness. The depinning field difference is highly dependent on the angle of the notch. This is attributed to the tilting of the Néel DW as it propagates through the nanowire. We also show via micromagnetic simulation that the damping constant plays a pivotal role in controlling the strength of the depinning field difference. Damping constant dependent behaviour is not reflected in our theoretical derivation due to the usage of energy arguments. This spin orientation dependent diode property could be exploited in magnetic memory or logic devices.

## 2. Theoretical model

An ultrathin nanowire with length  $l$ , width  $w$  and thickness  $t$  such that  $t \ll l$ ,  $w$  is considered. The  $x$  axis is along the wire length,  $y$  axis is along the width and  $z$  axis is along the

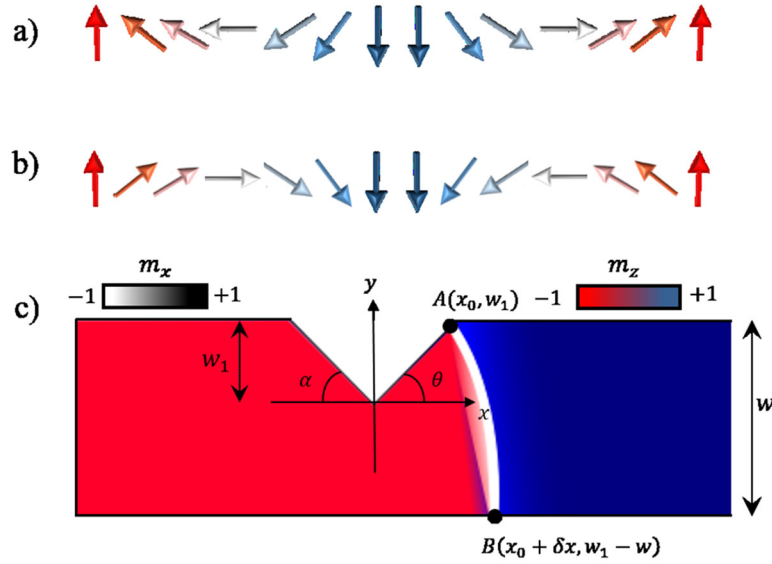


**Figure 1.** (a) Schematic for Néel DW profiles with right handedness. (b) Schematic for Néel DW profiles with left handedness. (c) Schematic of a notched nanowire of dimension  $l \times w \times t$ . A Néel DW is geometrically pinned at the triangular notch of depth  $w_1$  which extends an angle of  $\theta$  and  $\alpha$  from the  $x$ -axis.

thickness, out of plane. A triangular notch of  $w_1$  depth which extends an angle of  $\theta$  and  $\alpha$  along the  $x$ -axis is positioned at the top edge as shown in figure 1(c).

The total free energy of the notched nanowire can be described by:

$$\mathcal{E}(\mathbf{m}) = \int [\varepsilon_{\text{ex}}(\mathbf{m}) + \varepsilon_{\text{DM}}(\mathbf{m}) + \varepsilon_a(\mathbf{m}) + \varepsilon_d(\mathbf{m}) + \varepsilon_h(\mathbf{m})] dV, \quad (1)$$

where  $\mathbf{m}$  is the unit magnetization,  $\varepsilon_{\text{ex}}(\mathbf{m}) = A(\nabla\mathbf{m})^2$  is the exchange energy density with exchange constant  $A$ ,  $\varepsilon_{\text{DM}}(\mathbf{m}) = -D[m_z(\nabla \cdot \mathbf{m}) - (\mathbf{m} \cdot \nabla)m_z]$  is the Dzyaloshinskii–Moriya exchange energy density, the magnetization spatial variation along the  $z$ -direction is neglected ( $\partial\mathbf{m}/\partial z \approx 0$ ) due to an ultra-thin nanowire being considered,  $D$  is the parameter that takes into account the intensity of IDM interaction,  $\varepsilon_a(\mathbf{m}) = K_u[1 - (\mathbf{m} \cdot \mathbf{u}_k)^2]$  is the anisotropic energy density with  $K_u$  as the uniaxial anisotropy constant,  $\varepsilon_d(\mathbf{m}) = -\frac{1}{2}\mu_0 M_s \mathbf{m} \cdot \mathbf{h}_d$  is the demagnetizing energy density, and  $\varepsilon_h(\mathbf{m}) = -\mu_0 M_s \mathbf{m} \cdot \mathbf{h}$  is the Zeeman energy density.

Using calculus of variation to minimize the energy in equation (1) with constraint  $\mathbf{m} \cdot \mathbf{m} = 1$ , yields the Euler-Lagrangian equation,

$$\frac{d}{dt} \left( \frac{\delta \mathcal{E}}{\delta \dot{m}_i} \right) - \frac{\delta \mathcal{E}}{\delta m_i} = 2\lambda m_i, \quad (2)$$

where  $i = 1, 2, 3$ . In the presence of IDM interaction, boundary condition

$$\frac{\partial \mathbf{m}}{\partial \mathbf{n}} = \frac{D}{2A} \mathbf{m} \times (\mathbf{n} \times \mathbf{u}_z), \quad (3)$$

where  $\mathbf{n}$  is a local unit vector perpendicular to the nanowire surface that has to be imposed on solutions to equation (2). If equation (2) has a DW solution with non-zero external field  $\mathbf{h}$ , this implies that the DW is pinned within the system. The geometrical constriction can be treated as a trap potential well for

DW [25] and the pinning function can be assumed phenomenologically to approximate the true pinning potential around a notch. Recently, a criterion valid for all DWs and notches in a system without DM interaction was derived to estimate static DW depinning field [26]. However, no explicit form of the pinning potential was assumed. To derive the difference of depinning field in our system, we consider a more general form of the criterion,

$$\int_{\partial\Omega} (\nabla \cdot m_i) \nabla m_i d\mathbf{S} = \int_{\partial\Omega} \varepsilon^* d\mathbf{S} - \int_{\Omega} \mathbf{h}_d \cdot \nabla \mathbf{m} dV, \quad (4)$$

where  $\varepsilon^*$  is the total energy density without demagnetizing energy density term,  $\partial\Omega$  is the boundary of the nanowire. With the presence of IDM interaction in a magnetic system with perpendicular anisotropy, the Néel DW is favoured as the stable magnetization texture. Subsequent discussion is based on a Néel DW in a notched nanowire.

Without loss of generality, the case  $D < 0$  is considered as the case  $D > 0$  can be deduced by symmetry argument. For a system with  $D < 0$ , the Néel DWs adopt left-handed spin orientation as shown in figure 1(b): up–down  $\uparrow\downarrow$  (down–up  $\downarrow\uparrow$ ) magnetization with internal profile pointing along the negative (positive)  $x$ -axis. As shown in figure 1(c), Néel DW pinned away from a notch centre (A) will have its shape deformed such that the DWs intersect perpendicularly with the defect edge [27]. For simplicity, both configurations are assumed to have the same DW shape. To describe these Néel DW profiles at the notch (A) and at the uniform edge (B), the following ansatz is used:

$$m_x = \cos \theta \sin \phi(x) \quad (5a)$$

$$m_y = \sin \theta \sin \phi(x) \quad (5b)$$

$$m_z = \cos \phi(x), \quad (5c)$$

where

$$\phi(x) = 2 \tan^{-1} \left( \exp \frac{\sin \theta (y - y') + \cos \theta (x - x')}{\Delta} \right). \quad (6)$$

$\theta$  is the notch angle,  $\phi$  is magnetization angle with respect to the  $x - y$  plane,  $(x', y')$  is the position of the DW,  $\Delta$  represents the wall width parameter,  $n$  is an integer that enables the two types of walls (where  $\phi$  varies from 0 to  $\pm\pi$  or from  $\pm\pi$  to  $\pm 2\pi$ ). The  $\pm$  determines the handedness of the DW. Equation (6) can be reduced to the familiar 1D profile describing the domain profile at the uniform edge (B) by setting  $\theta \rightarrow 0$ . By applying equation (4) to both cases and since the exchange energy density, anisotropy energy density, demagnetizing energy density and the LHS term of equation (4) are essentially the same for both  $\uparrow\downarrow$  and  $\downarrow\uparrow$  configurations,

$$\int_{\partial\Omega} (\nabla \cdot \mathbf{m}_i^{\uparrow\downarrow}) \nabla m_i^{\uparrow\downarrow} d\mathbf{S} = \int_{\partial\Omega} (\nabla \cdot \mathbf{m}_i^{\downarrow\uparrow}) \nabla m_i^{\downarrow\uparrow} d\mathbf{S} \quad (7a)$$

$$\int_{\partial\Omega} \varepsilon_{\text{ex}}(\mathbf{m}_{\uparrow}) d\mathbf{S} = \int_{\partial\Omega} \varepsilon_{\text{ex}}(\mathbf{m}_{\downarrow}) d\mathbf{S} \quad (7b)$$

$$\int_{\partial\Omega} \varepsilon_a(\mathbf{m}_{\uparrow}) d\mathbf{S} = \int_{\partial\Omega} \varepsilon_a(\mathbf{m}_{\downarrow}) d\mathbf{S} \quad (7c)$$

$$\int_{\Omega} \mathbf{h}_d \cdot \nabla \mathbf{m}_{\uparrow} d\mathbf{V} = \int_{\Omega} \mathbf{h}_d \cdot \nabla \mathbf{m}_{\downarrow} d\mathbf{V} \quad (7d)$$

thus,

$$\int_{\partial\Omega} \Delta \varepsilon_h^* d\mathbf{S} = \int_{\partial\Omega} \Delta \varepsilon_{\text{DM}}^* d\mathbf{S} \quad (8)$$

where  $\Delta \varepsilon_h^* = \varepsilon_h(\mathbf{m}_{\uparrow}) - \varepsilon_h(\mathbf{m}_{\downarrow})$  is the difference in depinning field and  $\Delta \varepsilon_{\text{DM}}^* = \varepsilon_{\text{DM}}(\mathbf{m}_{\uparrow}) - \varepsilon_{\text{DM}}(\mathbf{m}_{\downarrow})$  corresponds to the difference in DM interaction energy density for  $\uparrow\downarrow$  and  $\downarrow\uparrow$  DW. A  $\uparrow\downarrow$  DW is considered to be positioned at the notch as  $A(x_0, w_1)$  and at the uniform edge as  $B(x_0 + \delta x, w_1 - w)$  respectively. In this calculation, the  $\uparrow\downarrow$  DW shape bending is assumed to be small.

For IDM interaction energy along a notch,

$$E_{\text{DM}}^{\text{notch}} = -Dt \int_{\partial\Omega} \left( m_x \frac{\partial m_z}{\partial x} - m_z \frac{\partial m_x}{\partial x} + x \rightarrow y \right) ds. \quad (9)$$

Substituting the DW profile along with its derivatives, and noting that  $\partial m_i / \partial x_j \approx 0$  for the region away from the DW,

$$E_{\text{DM}}^{\text{notch}} = 4Dt \tan^{-1} \left( \tanh \left( \frac{\sec \theta}{4} \right) \right). \quad (10)$$

At the uniform edge (B), the IDM interaction energy can be obtained by repeating a similar procedure. The IDM interaction energy of the system is then found to be

$$E_{\text{DM}}^{\uparrow\downarrow} = 4Dt \left[ \tan^{-1} \left( \tanh \left( \frac{\sec \theta}{4} \right) \right) - \tan^{-1} \left( \tanh \left( \frac{1}{4} \right) \right) \right]. \quad (11)$$

The IDM interaction energy for the  $\downarrow\uparrow$  DW configuration can be computed in a similar manner. The difference in IDM interaction energy is determined to be  $2E_{\text{DM}}^{\uparrow\downarrow}$ . The calculation of

external field energy term is more straightforward compared to IDM interaction energy calculation. In this case, we will assume that  $\delta x$  is small such that our external field energy term is approximately

$$E_h \approx \mu_0 M_s t h_c^{\uparrow\downarrow} (2w + 2w_1 (\text{cosec} \theta - \cot \theta)). \quad (12)$$

The difference in external field energy between the two Néel DWs is then found to be

$$\Delta E_h = 2\mu_0 M_s \Delta h_c t (w + w_1 (\text{cosec} \theta - \cot \theta)) \quad (13)$$

where  $|\Delta h_c| = |h_c^{\downarrow\uparrow} - h_c^{\uparrow\downarrow}|$ . Thus, the difference in depinning field for a symmetrical triangular notch is derived to be

$$|\Delta h_c| \approx \frac{4|D|}{\mu_0 M_s w} \left[ \tan^{-1} \left( \tanh \left( \frac{\sec \theta}{4} \right) \right) - \tan^{-1} \left( \tanh \left( \frac{1}{4} \right) \right) \right] \left( 1 + \frac{w_1}{w} (\text{cosec} \theta - \cot \theta) \right)^{-1}. \quad (14)$$

Equation (14) gives the analytical estimate for the difference in static depinning field for Néel DWs of the same handedness that occurs in a symmetric triangularly notched nanowire. From equation (14), it can be observed that as long as IDM interaction is present in a notched modulated nanowire, a depinning anomaly exists. This is because the only possible way to have  $\Delta h_c = 0$ , we would need  $\theta = 0$  which corresponds to a uniform nanowire. For an asymmetrical triangular notch, the last term of equation (14) is modified as  $\left[ 1 + \frac{w_1}{2w} ((\text{cosec} \theta - \cot \theta) + (\text{cosec} \alpha - \cot \alpha)) \right]^{-1}$ , where  $\theta$  and  $\alpha$  are the notch angles. An expression for a rectangular notch of depth  $w_1$  and width  $l_1$  can be also derived by substituting  $\theta = \pi/2$  in equation (14). In this case, the governing equation is reduced to

$$|\Delta h_c| \approx \frac{4|D|}{\mu_0 M_s w} \left[ \frac{\pi}{4} - \tan^{-1} \left( \tanh \left( \frac{1}{4} \right) \right) \right] \left( 1 + \frac{w_1}{w} \right)^{-1}. \quad (15)$$

The equations derived above are based on the following assumptions: (1) the magnetization is uniform along the thickness direction which is only valid if the wire thickness is less than exchange length  $\Delta$ . This assumption leads the derived depinning field to be thickness independent. In a real system where stable DW texture is dependent on film thickness [28, 29], wire thickness is an important parameter in determining the depinning field. (2) In our calculation, we assume that the  $\uparrow\downarrow$  and  $\downarrow\uparrow$  DW acquire the same shape when they are marginally pinned as shown in figure 1(c). As a first approximation, unconstrained Néel DW profiles are used to model the DWs along the edges of the nanowire. In reality, with the presence of DM interaction, field driven DW will exhibit tilting that is dependent on the DW profile [20], thus we will have different DW shapes for the spin orientations considered. However, as will be shown in a subsequent section, such an approximation is still good enough to capture the depinning anomaly dependence on the geometrical property of a system.

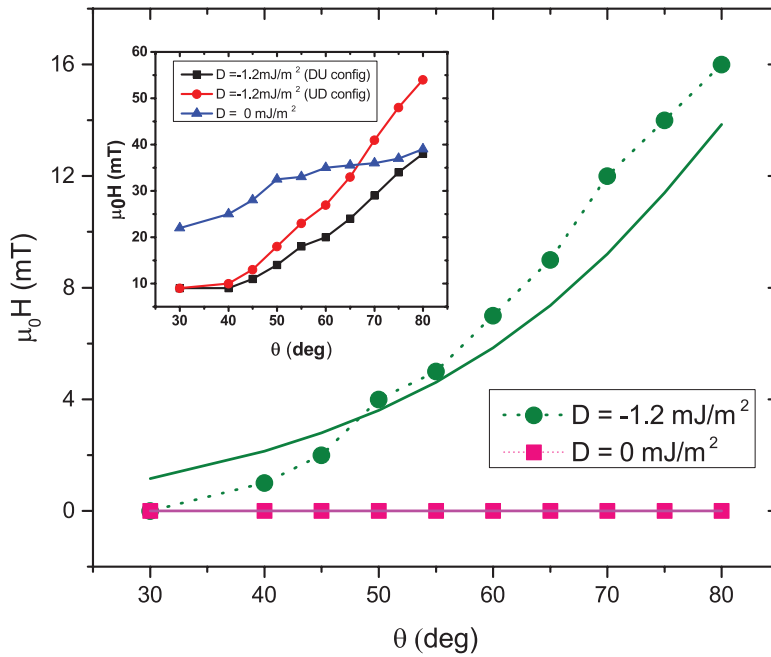


**Figure 2.** Difference in depinning field for  $\downarrow\uparrow$  and  $\uparrow\downarrow$  DW configuration as a function of notch angle  $\theta$ . Dots are the results of micromagnetic simulations, the continuous lines are the results of the theoretical estimates. The inset shows the depinning field of the aforementioned DW configurations for  $D = 0$  and  $-1.2\text{ mJ m}^{-2}$ .

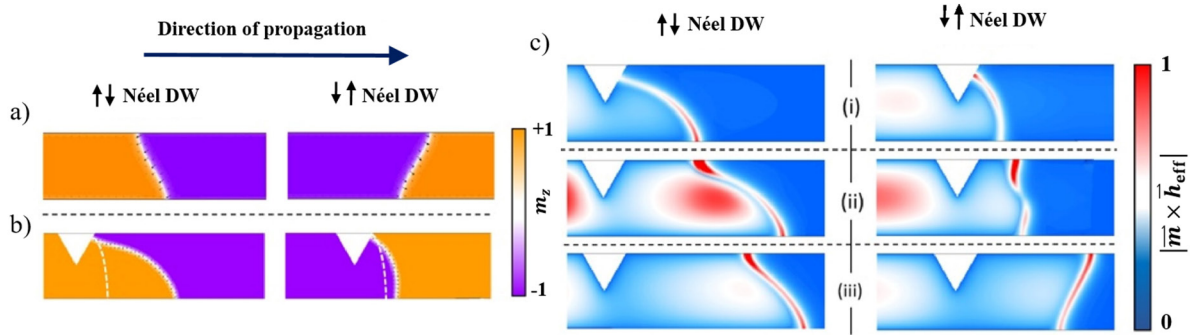
### 3. Numerical validation

In this section, the analytical predictions are compared with numerical results and the validity of the theoretical model is discussed. The OOMMF simulation package [30] is used to perform the magnetization dynamics simulations. In the simulations, all nanowires are 2500nm long, 160nm wide and 3nm thick. The triangular notch is positioned at the centre of the nanowire with varying notch depth  $w_1$  and notch angle  $\theta$ . The sample is discretized into  $2 \times 2 \times 3 \text{ nm}^3$ . The nanowire is parametrized with  $A = 1 \times 10^{-11} \text{ J m}^{-1}$ ,  $M_s = 7 \times 10^5 \text{ A m}^{-1}$ ,  $K_a = 4.8 \times 10^5 \text{ J m}^{-3}$  and  $D = -1.2 \times 10^{-1} \text{ J m}^{-2}$ . The damping constant  $\alpha$  is taken to be 0.3. A Néel DW is initially positioned at the centre of the notch. An external field is applied along the  $z$  direction in steps of 1 mT until the DW is completely depinned from the notch. The minimum static depinning field is denoted as  $h_c^{\downarrow\uparrow}$  for  $\downarrow\uparrow$  configuration and  $h_c^{\uparrow\downarrow}$  for  $\uparrow\downarrow$  respectively. The difference in static depinning field is obtained via  $|\Delta h_c| = ||h_c^{\downarrow\uparrow}| - |h_c^{\uparrow\downarrow}|$ . The difference in static depinning field is studied as a function of wire width for a fixed notch angle and as a function of notch angle for fixed width.

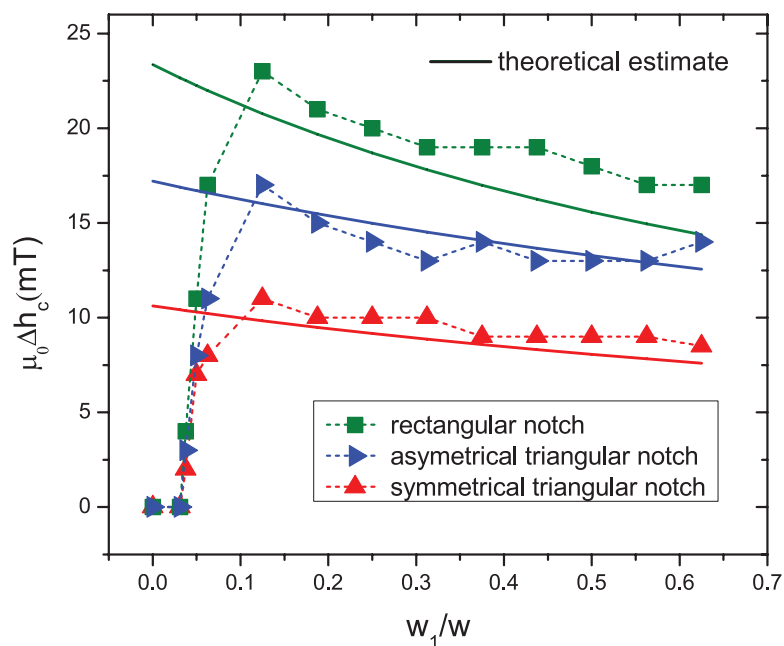
Figure 2 shows  $\Delta h_c$  as a function of notch angle  $\theta$  with  $w_1/w$  set as 0.5 for  $D = 0$  and  $-1.2 \text{ mJ m}^{-2}$ . For the case  $D = 0$ , the depinning anomaly vanishes. This confirms our theoretical prediction that the IDM interaction is responsible for the difference in static depinning field observed in Néel DW configuration with similar handedness. For notched nanowire with DM interaction, our simulation indicates that the difference in static depinning field increases with an increase in notch angle. In both cases, our theoretical estimate is in good agreement with numerical results. For low angles, the discrepancy between the numerical results and theoretical estimates arises due to the assumption made in the theoretical derivation, i.e.

we consider the DW deformation profile for both  $\downarrow\uparrow$  and  $\uparrow\downarrow$  magnetization to be the same as shown in figure 1. In reality, such assumption is a good approximation only for  $\downarrow\uparrow$  configuration, as the  $\uparrow\downarrow$  configuration will have its DW deformed significantly as shown in figure 3(b).

The depinning anomaly can be understood from the tilting of Néel DW which is induced by the IDM interaction. When driving the  $\downarrow\uparrow$  ( $\uparrow\downarrow$ ) Néel DW along  $+x$  direction, the DW will be tilted such that the top (bottom) edge DW leads the bottom (top) edge DW as shown in figure 3(b). In a notched nanowire where the  $\downarrow\uparrow$  DW is pinned at the edge of the notch, the leading DW will need to overcome the pinning potential before adopting the tilted DW structure as seen in uniform nanowire in its subsequent motion. On the other hand, when driving the  $\uparrow\downarrow$  Néel DW configuration along  $+x$  direction, the DW will have its leading (trailing) DW at the bottom (top) edge. Thus for this case, the leading DW does not experience any pinning potential of the notch and is allowed to adopt its shape similar to the one in uniform nanowire except with its trailing DW experiencing pinning potential. Figures 3(c)(i)–(iii) show the normalised torque exerted on the DW by effective field  $h_{\text{eff}}$  which is represented in color map. As the DWs propagate, the magnetization on the left of the DW undergoes relaxation and experiences non-zero torque from the effective magnetic field, whereas the magnetization on the right of the DW experiences vanishingly small torque. Prior adopting a tilted DW configuration that transverses with constant velocity, the leading DW will have a larger torque acting on it compared to the trailing DW. This implies that for a given fixed pinning potential, we would need a larger external field to produce the required torque to detach the  $\uparrow\downarrow$  DW from the notch as compared to  $\downarrow\uparrow$  DW. This is consistent with the numerical results shown in the inset of figure 2 where the static depinning field of  $\uparrow\downarrow$  DW has a large value compared to  $\downarrow\uparrow$  DW.



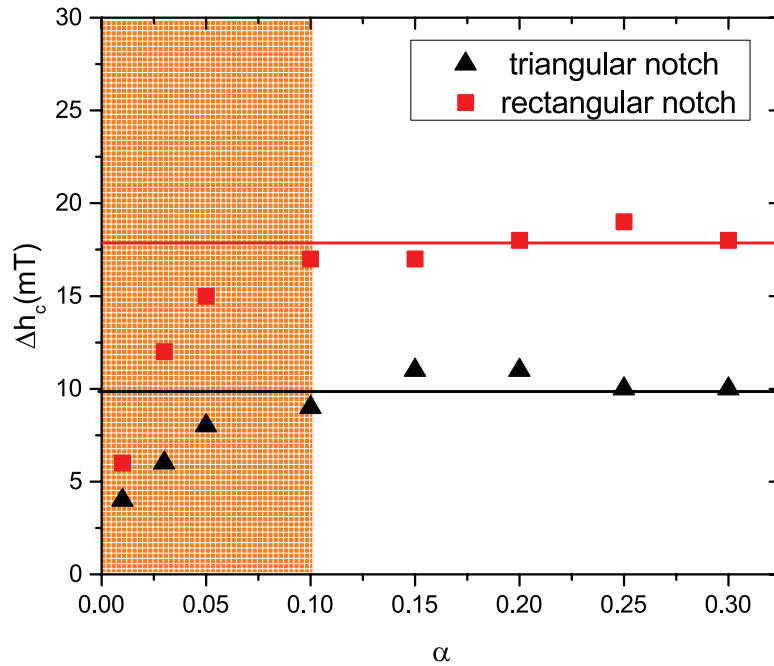
**Figure 3.** (a) Tilting of Néel DW surface for both  $\downarrow\uparrow$  and  $\uparrow\downarrow$  configuration, (b) Néel DW shape adopted when it is marginally pinned. Dashed line indicates the Néel DW deformation profile assumed in our theoretical derivation. (c) (i)–(iii) Normalized torque acting on the Néel DW structure by the effective field during the depinning process. For  $\downarrow\uparrow$  ( $\uparrow\downarrow$ ) DW configuration, the top (bottom) DW initially experiences a larger torque compared to the bottom (top) DW.



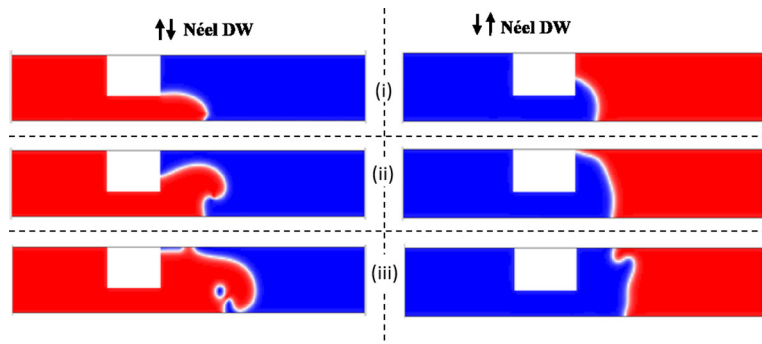
**Figure 4.** Difference in depinning field for  $\downarrow\uparrow$  and  $\uparrow\downarrow$  DW configuration as a function of  $w_1/w$  for a symmetrical triangular notch ( $\theta = \alpha = 65^\circ$ ), an asymmetrical triangular notch ( $\theta = 75^\circ$ ,  $\alpha = 45^\circ$ ) and a rectangular notch ( $\theta = \alpha = 90^\circ$ ). Dots are the results of micromagnetic simulations, the continuous lines are the results of the theoretical estimates.

Figure 4 depicts  $\Delta h_c$  as a function of notch width  $\theta$  for asymmetrical triangular notch, symmetrical notch and rectangular notch. The numerical data for  $w_1/w$  above 0.1 agrees with the theoretical estimate: the depinning field increases with decreasing  $w_1/w$ . The intuitive picture for the depinning field difference is related to the distance between the pinning site and the lower edge of the wire. Due to the DW tilting induced by the IDM, the leading edge of the DW, on the upper edge of the wire, will encounter the notch. For a fixed tilt DW angle, the lateral distance between the top edge of the DW at the notch and the lower edge of the DW at the wire will depend on the depth of the notch. The larger the depth of the notch, the smaller the lateral distance between the leading and trailing edge of the DW. As such, the depinning field difference is lower for larger depth. When the lateral distance between the two leading and trailing edge of

the DW increases, the depinning field difference increases. That is why for low  $w_1/w$  ratio, the theoretical trend shows an increase in the depinning field difference. The maximum lateral distance between the two DW edges will occur for the case of no notch in the wire. This may explain why theoretical estimate gives a finite value for  $w_1/w = 0$  and this value is maximum. For  $w_1/w < 0.1$ , the depinning field difference decreases significantly. Such a trend is not replicated by the theoretical estimate. This is due to several assumptions made in our derivation. As such, our equation is only valid for  $w_1/w > 0.1$ . One may observe that difference in static depinning field is insensitive to the variation of  $w_1/w$  ratio for a fixed notch angle. When the  $w_1/w$  is varied from 0.2 to 0.6,  $\Delta h_c$  is changed only by 2 mT. This is an attractive feature for logic or memory application, as the variation of notch width does not affect the depinning efficiency greatly.



**Figure 5.** Difference in depinning field as a function of Gilbert damping parameter  $\alpha$  for triangular notch and rectangular notch. The solid lines are theoretical estimates for triangularly notched nanowire and rectangularly notched nanowire respectively.



**Figure 6.** The evolution of DW during the depinning process with damping parameter  $\alpha = 0.05$ . The DWs is seen to undergo significant distortion and can no longer be treated as a rigid body.

#### 4. Effect of damping parameter $\alpha$ on depinning process

In our previous numerical simulations, a fixed damping constant of 0.3 is chosen. A good agreement is found between theoretical and simulation results. In this section, we show that the theoretical estimates derived in the previous section based on energy arguments fits only a selected range of  $\alpha$ . Figure 5 depicts the depinning field difference as a function of  $\alpha \leq 0.3$  for both triangular and rectangular notches. For  $\alpha \geq 0.1$ , the depinning field difference is fairly constant irrespective of the type of notch. For  $\alpha < 0.1$ , the difference in depinning field increases monotonically as a function of  $\alpha$ . As  $\alpha$  approaches zero, the depinning field difference between the different notch types becomes similar. Micromagnetic simulations reveal that the DW depinning dynamics for low  $\alpha$  exhibit considerable distortion as shown in figure 6. In our theoretical derivation, we assume the DW to be fairly rigid. The premature merging of DW and annihilation of domain at the nanowire edge as shown in figure 6(iii) is not taken into consideration.

This assumption is only true when the damping constant is sufficiently high to inhibit excessive spin precession. Thus, our theoretical estimate is only valid for  $0.1 \leq \alpha \leq 0.3$ .

We also study the depinning field of a DW in a rectangularly notched nanowire with varying  $\alpha$  from 0.01 to 1 as shown in figure 7. It is seen that the depinning field for  $\downarrow\uparrow$  DW is insensitive to the changes of  $\alpha$  in the high damping regime ( $\alpha > 0.4$ ). The depinning field for  $\downarrow\uparrow$  DW only reaches a constant value when the damping parameter  $\alpha$  is 1.0. Also, the depinning field difference vanishes when the damping parameter approaches 1.0. To understand the underlying depinning mechanism, we have plotted figures 8 and 9 showing the torques exerted on DWs. From figure 8,  $\downarrow\uparrow$  DW experiences greater torque at the top edge when the damping parameter is small. This torque facilitates the depinning of DW from the notch. When a large damping parameter is used, it results in a fast relaxation of spin moments and smaller torque exerts on the DW as shown in figure 8. This leads to higher external field required to depin the DW from the notch. In the high damping parameter regime  $\alpha = 1$ , the torque exerted on the

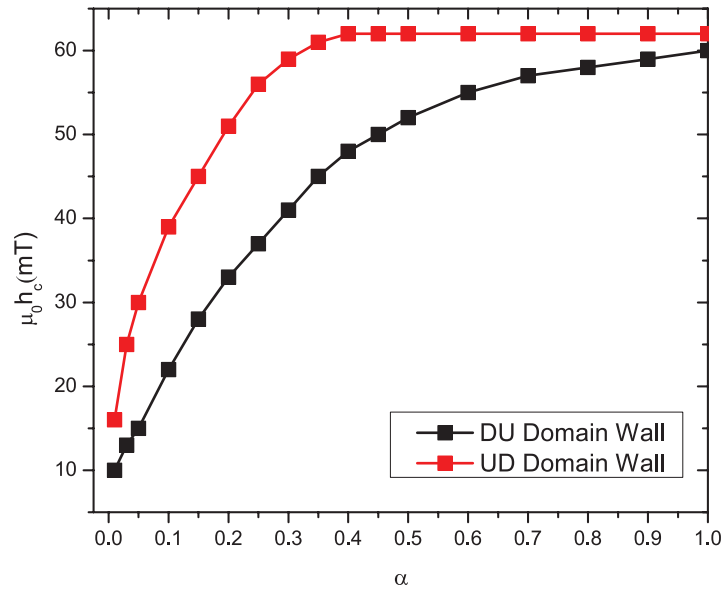


**Figure 7.** DWs’ depinning field as a function of Gilbert damping parameter  $\alpha$ . As  $\alpha$  approaches 1.0, the depinning field difference vanishes.

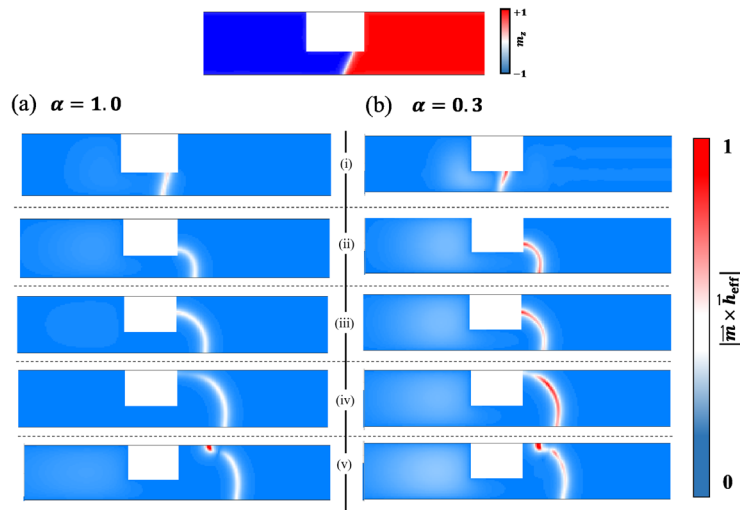


**Figure 8.** Normalised torque acting on  $\downarrow\uparrow$  DW by effective field during the depinning process with damping parameter  $\alpha = 0.3$  and 1.0. The normalisation is based on the maximum torque exerted on magnetization in the magnetic system with  $\alpha = 0.3$ .

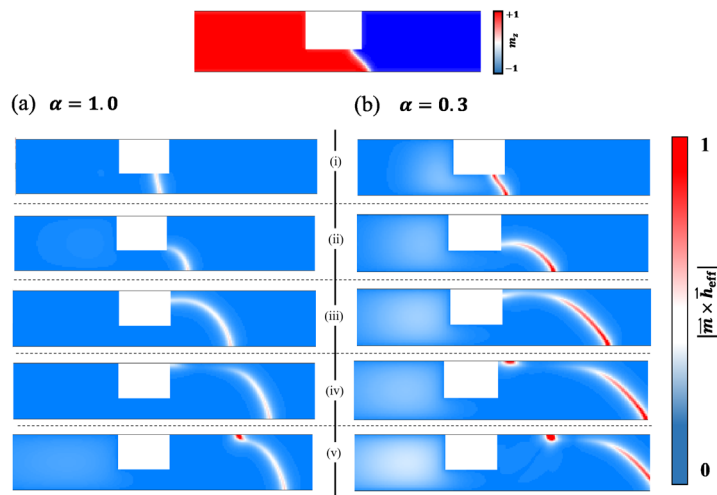


**Figure 9.** Normalised torque acting on  $\uparrow\downarrow$  DW by effective field during the depinning process with damping parameter  $\alpha = 0.3$  and 1.0. The normalisation is based on the maximum torque exerted on magnetization in the magnetic system with  $\alpha = 0.3$ .

$\uparrow\downarrow$  leading DW is of the same magnitude as  $\downarrow\uparrow$  trailing DW. While our theoretical estimate is able to account for the geometrical dependence of depinning anomaly but fails to capture the influence of damping parameter on the strength of depinning anomaly. For  $\alpha > 0.3$ , the damping term dominates the DW dynamics. Our derived theoretical estimates is unable to provide a satisfactory fit to the simulation results due to the absence of a damping term. The influence of the damping constant can be included by starting the derivation from the LLG equation.

## 5. Conclusion

To conclude, we demonstrate that the presence of Dzyaloshinskii–Moriya interaction leads to depinning anomaly in Néel DW with theoretical derivation and simulation results. The difference in depinning fields is highly dependent on the angle of the notch. Our results reveal that the minimum difference in depinning field occurs for symmetric triangular pinning sites. The derived theoretical estimate manages to explain the depinning anomaly for a particular range of damping constant where the assumption holds. The damping constant effect on depinning anomaly is explored.

## Acknowledgments

This work was supported by the Singapore National Research Foundation, Prime Minister’s Office, under a Competitive Research Programme (Non-volatile Magnetic Logic and Memory Integrated Circuit Devices, NRF-CRP9-2011-01), and an Industry-IHL Partnership Program (NRF2015-IIP001-001). The work was also supported by a MOE-AcRF Tier 2 Grant (MOE 2013-T2-2-017). WSL is a member of the Singapore Spintronics Consortium (SG-SPIN). We also wish to acknowledge the funding for this project from Nanyang Technological University under the Undergraduate Research Experience on Campus (URECA) programme.

## References

- [1] Parkin S S, Hayashi M and Thomas L 2008 *Science* **320** 190–4
- [2] Allwood D A, Xiong G, Faulkner C C, Atkinson D, Petit D and Cowburn R P 2005 *Science* **309** 1688–92
- [3] Goolaup S, Ramu M, Murapaka C and Lew W S 2015 *Sci. Rep.* **5** 9603
- [4] Hayashi M, Thomas L, Moriya R, Rettner C and Parkin S S 2008 *Science* **320** 209–11
- [5] Teoh H K, Goolaup S and Lew W S 2015 *IEEE Magn. Lett.* **6** 1–4
- [6] Dzyaloshinsky I 1958 *J. Phys. Chem. Solids* **4** 241–55
- [7] Moriya T 1960 *Phys. Rev.* **120** 91–8
- [8] Yang H, Thiaville A, Rohart S, Fert A and Chshiev M 2015 *Phys. Rev. Lett.* **115** 267210
- [9] Ryu K S, Thomas L, Yang S H and Parkin S 2013 *Nat. Nanotechnol.* **8** 527–33
- [10] Bode M, Heide M, Von Bergmann K, Ferriani P, Heinze S, Bihlmayer G, Kubetzka A, Pietzsch O, Blügel S and Wiesendanger R 2007 *Nature* **447** 190–3
- [11] Chen G, Ma T, N’Diaye A T, Kwon H, Won C, Wu Y and Schmid A 2013 *Nat. Commun.* **4** 2671
- [12] Hiramatsu R, Kim K J, Nakatani Y, Moriyama T and Ono T 2014 *Japan. J. Appl. Phys.* **53** 108001
- [13] Zang J, Mostovoy M, Han J H and Nagaosa N 2011 *Phys. Rev. Lett.* **107** 136804
- [14] Moon J H, Seo S M, Lee K J, Kim K W, Ryu J, Lee H W, McMichael R D and Stiles M D 2013 *Phys. Rev. B* **88** 184404
- [15] Rohart S and Thiaville A 2013 *Phys. Rev. B* **88** 184422
- [16] Fert A, Cros V and Sampaio J 2013 *Nat. Nanotechnol.* **8** 152–6
- [17] Heide M, Bihlmayer G and Blügel S 2008 *Phys. Rev. B* **78** 140403
- [18] Chen G et al 2013 *Phys. Rev. Lett.* **110** 177204
- [19] Je S G, Kim D H, Yoo S C, Min B C, Lee K J and Choe S B 2013 *Phys. Rev. B* **88** 214401
- [20] Boulle O, Rohart S, Buda-Prejbeanu L D, Jué E, Miron I M, Pizzini S, Vogel J, Gaudin G and Thiaville A 2013 *Phys. Rev. Lett.* **111** 217203
- [21] Thiaville A, Rohart S, Jué É, Cros V and Fert A 2012 *Europhys. Lett.* **100** 57002
- [22] Tretiakov O A and Abanov A 2010 *Phys. Rev. Lett.* **105** 157201
- [23] Yoshimura Y, Kim K J, Taniguchi T, Tono T, Ueda K, Hiramatsu R, Moriyama T, Yamada K, Nakatani Y and Ono T 2016 *Nat. Phys.* **12** 157–61
- [24] Sato K and Tretiakov O A 2016 *Appl. Phys. Lett.* **108** 122403
- [25] Ahn S M, Moon K W, Kim D H and Choe S B 2012 *J. Appl. Phys.* **111** 07D309
- [26] Yuan H Y and Wang X R 2014 *Phys. Rev. B* **89** 054423
- [27] Kim K J and Choe S B 2009 *J. Magn. Magn. Mater.* **321** 2197–9
- [28] Ramstöck K, Hartung W and Hubert A 1996 *Phys. Status Solidi A* **155** 505–18
- [29] Navas D, Redondo C, Confalonieri G A B, Batallan F, Devishvili A, Iglesias-Freire O, Asenjo A, Ross C A and Toperverg B P 2014 *Phys. Rev. B* **90** 054425
- [30] <http://math.nist.gov/oommf/>